

Research Paper

Exosomes from mesenchymal stem cells modulate endoplasmic reticulum stress to protect against nucleus pulposus cell death and ameliorate intervertebral disc degeneration in vivo

Zhiwei Liao*, Rongjin Luo*, Gaocai Li*, Yu Song, Shengfeng Zhan, Kangcheng Zhao, Wenbin Hua, Yukun Zhang, Xinghuo Wu, Cao Yang 

Department of Orthopaedics, Union Hospital, Tongji Medical College, Huazhong University of Science and Technology, Wuhan 430022, China

*These authors contributed equally to this work

 Corresponding author: Department of Orthopaedics, Union Hospital, Tongji Medical College, Huazhong University of Science and Technology, Wuhan 430022, China. E-mail address: caoyangunion@hust.edu.cn (C. Yang).

© Ivyspring International Publisher. This is an open access article distributed under the terms of the Creative Commons Attribution (CC BY-NC) license (<https://creativecommons.org/licenses/by-nc/4.0/>). See <http://ivyspring.com/terms> for full terms and conditions.

Received: 2019.01.30; Accepted: 2019.04.13; Published: 2019.05.31

Abstract

Objectives: Intervertebral disc degeneration (IDD) is widely accepted as a cause of low back pain and related degenerative musculoskeletal disorders. Nucleus pulposus (NP) cell apoptosis which is related to excessive endoplasmic reticulum (ER) stress in the intervertebral disc (IVD) could aggravate IDD progression. Many studies have shown the therapeutic potential of exosomes derived from bone marrow mesenchymal stem cells (MSC-exos) in degenerative diseases. We hypothesized that the delivery of MSC-exos could modulate ER stress and inhibit excessive NP cell apoptosis during IDD.

Methods: The ER stress levels were measured in normal or degenerative NP tissues for contrast. The effects of MSC-exos were testified in advanced glycation end products (AGEs) -induced ER stress in human NP cells. The mechanism involving AKT and ERK signaling pathways was investigated using RNA interference or signaling inhibitors. Histological or immunohistochemical analysis and TUNEL staining were used for evaluating MSC-exos therapeutic effects *in vivo*.

Results: The ER stress level and apoptotic rate was elevated in degenerative IVD tissues. MSC-exos could attenuate ER stress-induced apoptosis by activating AKT and ERK signaling. Moreover, delivery of MSC-exos *in vivo* modulated ER stress-related apoptosis and retarded IDD progression in a rat tail model.

Conclusions: These results highlight the therapeutic effects of exosomes in preventing IDD progression. Our work is the first to demonstrate that MSC-exos could modulate ER stress-induced apoptosis during AGEs-associated IVD degeneration.

Key words: Mesenchymal stem cells, exosomes, advanced glycation end products, endoplasmic reticulum stress, intervertebral disc degeneration

Introduction

Intervertebral disc degeneration (IDD) is considered as the leading cause of low back pain, resulting in a great burden on the global health care system [1]. The intervertebral disc (IVD) is composed of the inner nucleus pulposus (NP) and outer annulus fibrosus (AF), which functions as the load-bearing and buffering unit of the spine [2]. Located in the inner

disc, NP cells mainly produce and maintain the extracellular matrix (ECM). It is accepted that IDD progression is initiated and accelerated by the depletion of NP cells and degradation of ECM [3]. Inhibiting the apoptosis of NP cells during IDD could be an effective way to prevent or reverse disc degeneration.

Advanced glycation end products (AGEs) are formed by non-enzymatic reaction of reducing sugars with free amino groups of macromolecules, also called the Millard reaction [4]. AGEs usually accumulate in aging and degenerative tissues, and are closely related to inflammation, metabolic dysfunction and endoplasmic reticulum (ER) stress, especially in collagen-rich tissues [5-7]. AGEs can induce ER stress and then activate the unfolded protein response (UPR) through crucial transmembrane proteins in ER [4, 8, 9]. Initiated by the UPR, the C/EBP homologous protein (CHOP), a downstream growth arrest gene, is transcriptionally activated and controls the expression of apoptosis-related genes and induces cell apoptosis under severe ER stress [10]. CHOP has been verified as a crucial mediator in ER stress-induced apoptosis signaling [11-13]. A study showed that silencing of CHOP could inhibit AF cell apoptosis and ameliorate IDD in a rat model [14]. Accumulating evidence suggests that AGEs accumulate in IVD tissues and became a crucial mediator during IDD progression [15-17]. Previous studies also demonstrated that the deposition of AGEs elicits both inflammation and oxidative stress in IVD and promote the process of IDD [7, 18]. Accumulation of AGEs in organs or tissues induces severe ER stress and results in cell death through the UPR hyperactivation and downstream activation of caspases [4]. Consequently, inhibition of AGEs-induced ER stress could be a therapeutic target for IDD treatment.

Therapeutic methods for IDD focus on the restoration of apoptotic, damaged or aging NP cells, and mesenchymal stem cells (MSC) are considered as a potential choice for disc repair [3, 19, 20]. MSC transplantation ameliorates the progression of IDD partly through supplementing exhausted NP cells or attenuating excessive cell apoptosis during IDD [21]. Accumulating evidence has revealed the role of MSC paracrine factors in maintaining the proliferation and reducing the apoptosis of NP cells [22, 23]. Interestingly, MSCs are found to transfer specific types of extracellular vesicles, such as exosomes, to achieve their therapeutic paracrine effects [24]. MSC-derived exosomes are bilayer vesicles of 50-200 nm diameter, containing various cytokines, signaling proteins or lipids, and regulatory nucleic acids [25, 26]. Exosomes, a cell-free mediator, are involved in cell-to-cell communication, cell signaling and metabolism modulation, and play a crucial role in MSC-based therapy [27]. Transplantation of exosomes into target cells can alter cell signaling related to proliferation, differentiation, autophagy or apoptosis and many other cellular activities [28, 29]. However, the underlying mechanisms of exosomes-based

therapy are not fully understood and deserve to be further explored.

Our previous study has shown that AGEs accumulate in NP tissues and correlate with the Pfirrmann grades of IVD [18]. In the present study, we measured the expression levels of ER stress marker and UPR related gene in normal and degenerative NP tissues. The *in vitro* studies revealed that AGEs promoted NP cell apoptosis by inducing ER stress with the UPR activation, and exosomes derived from bone marrow MSC (MSC-exos) could attenuate the apoptotic rates in human NP cells. Moreover, we designed experiments and testified that MSC-exos could attenuate the AGEs-induced ER stress through activating AKT and ERK signaling pathways *in vitro*. Meanwhile, the therapeutic effect of MSC-exos injection on IDD was tested *in vivo* using a rat tail model. Our study offers new insights into the mechanisms of ER stress-related apoptosis in human NP cells and the application of MSC-exos as a therapy for IDD.

Materials and methods

NP cells isolation and culture

All the experimental protocols were approved by the Ethics Committee of Tongji Medical College, Huazhong University of Science and Technology. With informed consent from the patients, normal NP tissues were collected from patients (n = 15, 7 males and 8 females, aged 13-24 years, mean age 18.8 years) who underwent surgery for idiopathic scoliosis and degenerative NP tissues were obtained from patients (n = 15, 6 males and 9 females, aged 26-64 years, mean age 43.2 years) who underwent surgery for disc excision and spinal fusion surgery. The degenerative grade of human NP tissue samples was classified by the Pfirrmann grades according to magnetic resonance images of the patients as previously described [18]. Human NP tissues were cut into pieces and enzymatically digested in 0.2% type II collagenase (Gibco) and 0.25% trypsin (Gibco) for 3 h. After being filtered and washed in PBS, the suspension was centrifuged, and the isolated cells were cultured in Dulbecco's modified Eagle medium (DMEM) containing 15% fetal bovine serum (FBS) (Gibco) and 1% penicillin-streptomycin (Invitrogen). The culture medium was replaced twice every week and NP cells from the second or third passage were used in the following experiments.

Isolation and identification of mesenchymal stem cells

Human bone marrow specimens were harvested from the iliac crests of healthy volunteer donors. The

donors provided informed consent for their tissues to be used in this experiment. MSCs from bone marrow were isolated by density gradient centrifugation and adherence to tissue culture plastic. Cells were expanded in DMEM containing 15% FBS and 1% penicillin-streptomycin. The cells from the second or third passage were used in the following experiments. For the detection of cell surface markers, MSCs were characterized by positive expression of CD73, CD90 and CD105 and negative expression of CD34 and HLA-DR using flow cytometry (BD Biosciences, USA) according to the manufacturer's instructions. Fluorescein isothiocyanate (FITC)-labeled anti-human CD90, CD105, and phycoerythrin (PE)-labeled anti-human CD73, CD34, HLA-DR were all purchased from BD Biosciences. Moreover, the multi-lineage differentiation potential of MSCs was determined in osteogenic, chondrogenic, and adipogenic differentiation mediums, respectively (Cyagen, China). After cells were cultured in respective induction mediums according to standard protocols, Alizarin red staining, Oil red O staining and Alcian blue staining were performed to confirm each lineage differentiation, respectively.

Exosomes isolation and characterization

MSCs were cultured in DMEM deprived of FBS for 2 days. Then the culture media were harvested and centrifuged at 500 g for 10 min, 2000 g for 30 min to remove dead cells and debris, then 10000 g for 1 h to remove large vesicles. Next, we transferred the supernatant containing cell-free culture media to a new tube without disturbing the pellet and added the Total Exosome Isolation reagent (Invitrogen) in strict accordance with the manufacturer's instructions. After collecting the isolated exosomes, morphology was observed using Transmission Electron Microscopy (TEM) (FEI Tecnai G20 TWIN), and the number and size distribution of exosomes were analyzed by nanoparticle trafficking analysis (NTA) using the NANOSIGHT NS300 system (Malvern, UK) according to manufacturer's instructions. The particles were characterized by the expression of exosomal markers, such as Alix, TSG101, and CD63 using Western blot analysis.

Uptake of exosomes by NP cells

Purified MSC-exosomes were incubated with PKH26 (Sigma-Aldrich) for 5 min at room temperature. After washed in PBS and centrifuged at 110000 g for 90 min, the exosomes were suspended in basal medium and incubated with NP cells for 12 h at 37 °C. Then stained by 0.1 g/mL 4-6-diamidino-2-phenylindole (DAPI) (Beyotime, Nantong, China) for 5 min, the NP cells were placed under a fluorescence

microscope (Olympus, BX53; Melville, NY, USA) for image capture.

Western blot analysis

Total proteins were isolated using a protein extraction kit (Beyotime, Nantong, China) according to standard protocols. The antibodies used were: CD63 (1:1000), TSG101 (1:1000), Alix (1:1000), GRP78 (1:2000), GRP94(1:1000), CHOP (1:1000), caspase-3 (1:500), caspase-12 (1:1000) (Proteintech), p-PERK (1:1000), PERK (1:1000), ATF6 (1:1000), p-IRE1 α (1:1000), IRE1 α (1:1000) (Abcam), ERK (1:1000), p-ERK (1:1000), AKT(1:1000), p-AKT (1:1000), and GAPDH (1:1000) (Cell Signaling Technology). Horseradish peroxidase (HRP) -conjugated secondary antibodies (Santa Cruz Biotechnology) were used and protein bands were visualized and detected using an enhanced chemiluminescence system. GAPDH was used for normalization. The experiments were performed in triplicate.

Quantitative real-time polymerase chain reaction (qRT-PCR)

Total RNA was extracted with Trizol reagent (Invitrogen) from NP tissues and cultured cells, reverse-transcribed and amplified by qRT-PCR according to manufacturer's instructions. The primers used for qRT-PCR were as follows: Homo GRP78, forward 5'-CATCACGCCGTCCTATGTCG-3', reverse 5'-CGTCAAAGACCGTGTCTCG-3'. Homo CHOP, forward 5'-CCCTCACTCTCCAGATTCCAGTC-3', reverse 5'-CTAGCTGTGCCACTTTCCITTC-3'. Homo ATF4, forward 5'-CGAGGTGTTGGTGGGGG ACTTGA-3', reverse 5'- CAACCCATCCACAGCCA GCCATT-3'. Homo XBP1, forward 5'-AACCTGTA GAAGATGACCTCGTTC-3', reverse 5'-AAAGAGT TCATTGGCAAAGTGTC-3'. Homo GAPDH, forward 5'-TCAAGAAGGTGGTGAAGCAGG-3', reverse 5'-TCAAAGGTGGAGGAGTGGGT-3'. GAPDH was used for normalization. The experiments were performed in triplicate.

Immunofluorescence analysis

Immunofluorescence analysis was performed as previously described [30]. Briefly, NP cells or tissues attached to slides were fixed with 4% paraformaldehyde, then permeabilized with 0.2% Triton X-100 in PBS. The slides were washed in PBS and blocked with 2% bovine serum albumin (BSA) in PBS for 2 h at 37 °C, and then incubated with primary antibodies against: GRP78 (1:50), GRP94 (1:50), CHOP (1:100), caspase-3 (1:50), or caspase-12 (1:100) (Proteintech). After washed twice, the slides were subsequently treated with secondary goat anti-rabbit antibody (Boster) at 37 °C for 2 h. Nuclei were co-stained for 5 min with 0.1 g/mL DAPI (Beyotime,

Nantong, China), and images were captured under a microscope (Olympus, BX53; Melville, NY, USA).

Terminal deoxynucleotidyl transferase dUTP nick end labeling (TUNEL) staining

TUNEL staining was used to evaluate cell apoptosis. The cells were fixed in 4% paraformaldehyde for 1 h at room temperature and then treated with 0.5% TritonX-100 for 10 min. After washed with PBS, the cells were incubated with the cell death detection kit (Roche, Basel, Switzerland) according to the manufacturer's instructions. Nuclei were co-stained for 5 min with 0.1 g/mL DAPI (Beyotime, Nantong, China), and images were captured under a microscope (Olympus, BX53; Melville, NY, USA).

RNA interference

Knockdown of CHOP in NP cells was realized by transfected with short interfering RNA (siRNA). Si-RNA against CHOP (si-CHOP) and scrambled siRNA (si-NC) were synthesized by RiboBio (Guangzhou, China) and transfected with Lipofectamine 2000 (Invitrogen) according to the standard protocol. The sequences of siRNA were as follows: CHOP-homo-173, 5'-GCUGAGUCAUUGC CUUUCUTT-3' and 5'-AGAAAGGCAAUGACUCAG CTT-3'. CHOP-homo-247, 5'-GGUCCUGUCUUCAG AUGAATT-3' and 5'-UUCAUCUGAAGACAGGAC CTT-3'. CHOP-homo-520, 5'-GCGCAUGAAGAAG AAAGAATT-3' and 5'-UUCUUCCUUCUUCGCG CTT-3'. Si-NC, 5'-UUCUCCGAACGUCACGUTT-3' and 5'-ACGUGACACGUUCGGAGAATT-3'. After achieving high silencing efficiency, the NP cells were used in following treatment group.

Animal experiments

The animal experiments were conducted following a protocol approved by the Animal Experimentation Committee of Huazhong University of Science and Technology. A total of 25 three-month-old Sprague-Dawley rats were used for the *in vivo* experiments. Among them, 5 rats remained intact. After the animals were anesthetized with 2% (w/v) pentobarbital (40 mg/kg), three IVDs (Co7/8, Co8/9 and Co9/10) in each rat were located by palpation on the coccygeal vertebrae and confirmed by trial radiography. To evaluate the therapeutic effect of exosomes on IDD, three rat IVDs (Co7/8, Co8/9 and Co9/10) were underwent for the different treatments accordingly. More concretely, the three IVDs (Co7/8, Co8/9 and Co9/10) were accepted for intradiscal injection of PBS, AGEs (200 µg/mL) or a mixture of AGEs (200 µg/mL) and exosomes (100 µg/mL), respectively, at the same total injection volume (2 µL), using a 33-gauge needle (Hamilton,

Benade, Switzerland) [31, 32]. The injections were performed every two weeks for two months.

Histologic analysis

Animals were euthanized, and the discs were harvested. The specimens were decalcified and fixed in formaldehyde, dehydrated, then embedded in paraffin. The slides of each disc were stained with hematoxylin-eosin (HE) and assessed with a histological grading scale [33]. The sections were deparaffinized and rehydrated, and then microwaved in 0.01 mol/L sodium citrate for 15 min. Next, 3% hydrogen peroxide was used to block endogenous peroxidase activity for 10 min, and 5% bovine serum albumin was used to block nonspecific binding sites for 30 min. The sections were then incubated with primary antibody (CHOP, 1:100), (GRP78, 1:50), (caspase-3, 1:50) (Proteintech) overnight at 4 °C. Finally, the sections were incubated with an HRP-conjugated secondary antibody (Santa Cruz Biotechnology) and counterstained with hematoxylin. All tests were performed on at least three sections from each specimen.

Statistical analysis

Data are presented as the mean ± standard deviation of at least three independent experiments. Statistical analyses were performed using GraphPad Prism 7 software (La Jolla, CA, USA). Differences between group means were evaluated with Student's t-test or one-way ANOVA by analysis of variance. P-value < 0.05 shows a statistical significance.

Results

The expression of ER stress markers during the intervertebral disc degeneration

ER stress was related to the pathogenesis of IDD and severe ER stress could induce excessive apoptosis in NP cells [34, 35]. To ensure whether ER stress was relevant to the progression of IDD, the expression levels of ER stress markers were evaluated in NP samples at different degenerative degrees. The NP samples included 8 at Grade II, 7 at Grade III, 8 at Grade IV and 7 at Grade V according to the Pfirrmann grades [18]. The histological degenerative degrees of NP tissues were measured by HE, Alcian blue, and Masson staining (Fig. 1A). A marker for ER stress, GRP78, and a downstream protein initiated by the UPR, CHOP, were measured by western blot analysis in all NP tissue samples (Fig. 1B-D). In addition, the expression levels of GRP78 and CHOP were detected by qRT-PCR in all specimens (n = 30). Increasing levels of GRP78 and CHOP expression were found to positively correlate with Pfirrmann grades of IDD (Fig. 1E-F). Immunofluorescence analysis showed that

the levels of caspase-3 and caspase-12 expression were higher in the degenerative NP tissue samples compared with normal samples (Fig. 1G-H). These

results indicate that ER stress marker expression and ER stress-related apoptosis increase during the progression of IDD.

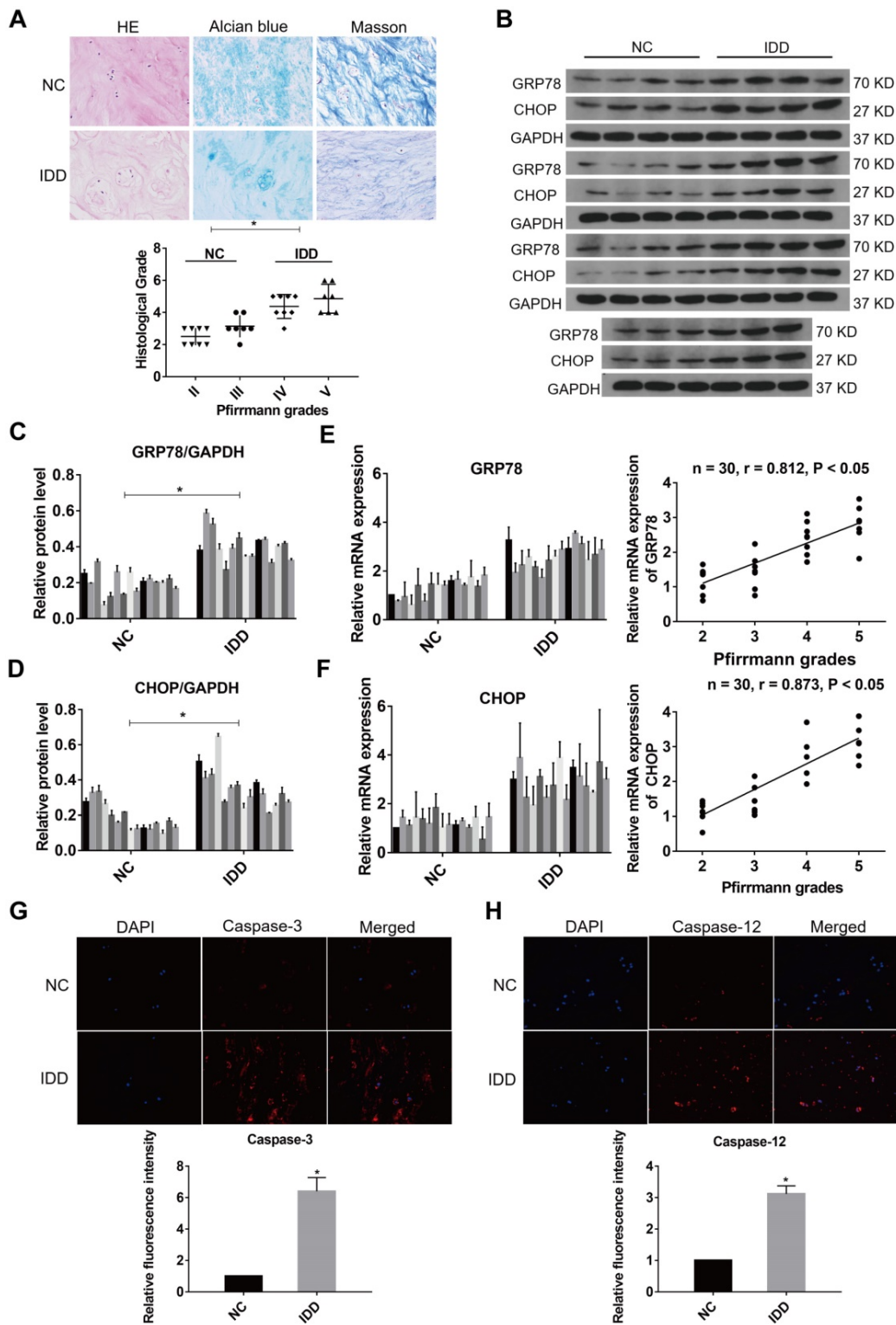


Figure 1. ER stress level during IDD in human NP tissues. (A) Representative histological images of normal or degenerative NP tissues in HE, Alcian blue and Masson staining. Magnification: 400 ×. Histological grades of NP tissues were evaluated and analyzed. *P < 0.05. (B-D) The protein levels of GRP78 and CHOP were analyzed by western blot analysis (B) and the relative quantitative data (C, D) was calculated accordingly. GAPDH was used as an internal control. *P < 0.05 vs NC group. (E) GRP78 mRNA level was measured by qRT-PCR in normal and degenerative NP tissues (left panel). A correlation between GRP78 mRNA level and Pfirrmann grades of NP tissues (n = 30) was determined by nonparametric linear regression (right panel). (F) CHOP mRNA level was analyzed by qRT-PCR (left panel) and linear regression confirmed a correlation between CHOP mRNA level and Pfirrmann grades of NP tissues (n = 30) (right panel). (G-H) Representative images of caspase-3 (G) and caspase-12 (H) expression was detected by immunofluorescence analysis and the relative fluorescence intensity was calculated in normal and degenerative NP tissues. Magnification: 400 ×. *P < 0.05 vs NC group.

Identification of MSC-exos and internalization by NP cells

Human MSCs were collected from the bone marrow aspirates of donors. Human MSCs were identified with a spindle-like appearance at about 60-70% confluence (Fig. 2A). MSCs were cultured in osteogenic, adipogenic or chondrogenic medium to induce the multilineage differentiation, respectively (Fig. 2B). Flow cytometry analysis showed that MSCs were positive for the surface antigens CD73, CD90 and CD105, and negative for CD34 and HLA-DR (Fig. 2C). MSC-derived exosomes (MSC-exos) were isolated and purified from MSC culture medium. Nanoparticle trafficking analysis (NTA), transmission electron microscopy (TEM) and western blotting were used to characterize the diameter, morphology and protein markers of MSC-exos, respectively. The concentration of exosomes was 5.72×10^8 particles/mL and the mean diameter of particles was 94.3 nm as measured by the NTA system (Fig. 2D). A relative intensity three-dimensional plot showed a stereo picture of the size distribution (Fig. 2E). The morphology of these particles was confirmed in the TEM image (Fig. 2F). According to the western blotting results, the levels of exosomal marker proteins such as Alix, TSG101, CD63 were much higher in exosomes than cells (Fig. 2G). Moreover, PKH26-labeled exosomes were incubated with NP cells in order to determine the exosomes engulfment by NP cells. As shown in Fig. 2H, fluorescence-labeled exosomes were distributed throughout the cytoplasm of NP cells under fluorescent microscopy, indicating that the nano-sized vesicles were internalized by NP cells.

MSC-exos reduced AGEs-induced ER stress and ameliorated NP cells apoptosis

AGEs are thought to have detrimental effects on cells through inducing severe ER stress and excessive apoptosis [5, 8]. Exosomes from stem cells have been indicated as anti-apoptotic in various conditions and could be applied to regulating cell apoptotic events [22, 24]. To assess the effects of MSC-exos on the NP cells, we treated NP cells with 10, 50, or 100 $\mu\text{g/mL}$ MSC-exos under AGEs (200 $\mu\text{g/mL}$) stimulation for 24 h. Then, the expression levels of ER stress markers GRP78 and GRP94 were analyzed by western blot, and the quantitative protein levels were calculated (Fig. 3A). Immunofluorescence analysis also showed that GRP78 or GRP94-labeled cells were increased in the AGEs group and decreased significantly when co-treated with MSC-exos (Fig. 3B-C). It was indicated that MSC-exos could ameliorate AGEs-induced ER stress in a dose-dependent manner. Since severe ER stress could cause cell apoptosis, we next compared

the activation level of caspase-3 and caspase-12 between the different groups (Fig. 4A). Caspase-3-labeled or caspase-12-labeled cells increased in the AGEs treatment group and decreased when co-treated with MSC-exos (Fig. 4B-C). TUNEL analysis also suggested that the apoptosis rate was increased under AGEs treatment and decreased in the MSC-exos group in a dose-dependent manner (Fig. 4D-E). Taken together, these results reveal that AGEs augment ER stress in human NP cells and treatment with MSC-exos exerts a protective effect by reducing ER stress-induced apoptosis.

MSC-exos inhibited the activation of UPR under AGEs-induced ER stress in human NP cells

It was previously shown that severe or prolonged ER stress induced the over-activation of the UPR, resulting in excessive protein degradation and ultimately cell death [11]. To further investigate the role of MSC-exos in AGEs-induced ER stress, we determined whether MSC-exos treatment could regulate the UPR activation. The expression of three transmembrane proteins in the classical branches of the UPR, protein kinase-like endoplasmic reticulum kinase (PERK), inositol-requiring protein 1 α (IRE1 α), and activating transcription factor 6 (ATF6) were measured by western blot analysis (Fig. 5A). As expected, AGEs treatment induced increased expression of ATF6, phosphorylated IRE1 α (p-IRE1 α) and phosphorylated PERK (p-PERK), which indicated activation of the UPR (Fig. 5B). The transcription of UPR target genes, activating transcription factor 4 (ATF4) and X-box binding protein 1 (XBP1) also increased accordingly (Fig. 5B-D). Moreover, a mediator of ER stress-related apoptosis, CHOP, was activated in transcription and protein levels under AGEs treatment (Fig. 5E). Interestingly, the expression of the downstream effectors ATF4, XBP1, and CHOP were all decreased significantly in the MSC-exos group compared with the AGEs group. Consequently, these data show that MSC-exos regulate the UPR activation in response to AGEs-induced ER stress in human NP cells.

MSC-exos attenuated AGEs-induced ER stress-induced apoptosis through CHOP regulation in human NP cells

Growing evidence has shown that the increased expression of CHOP could result in IVD cell apoptosis [14]. To confirm the relationship between CHOP and ER stress-related apoptosis, the effects of CHOP silencing in human NP cells were tested. CHOP silencing was realized by RNA interference and the silencing efficiency was measured at protein levels

(Fig. 6A) and transcriptional levels (data did not show). Silencing of CHOP or treatment with MSC-exos both significantly reduced caspase activation under the AGEs stimulation. When NP cells in the si-CHOP group were co-treated with MSC-exos (100 µg/mL), the inhibition of AGEs-induced caspases activation was even more apparent (Fig. 6B-F). Immunofluorescence analysis indicated that caspase-3 and caspase-12-labeled cells were decreased

significantly in the si-CHOP group with or without MSC-exos, compared with the si-NC group (Fig. 6F). Moreover, the TUNEL analysis results were consistent with the observations on caspase-3 and caspase-12 activation levels (Fig. 6G-H). Together, these data reveal that MSC-exos reduced the ER stress through the regulation of CHOP expression and attenuate ER stress-induced apoptosis under the AGEs treatment.

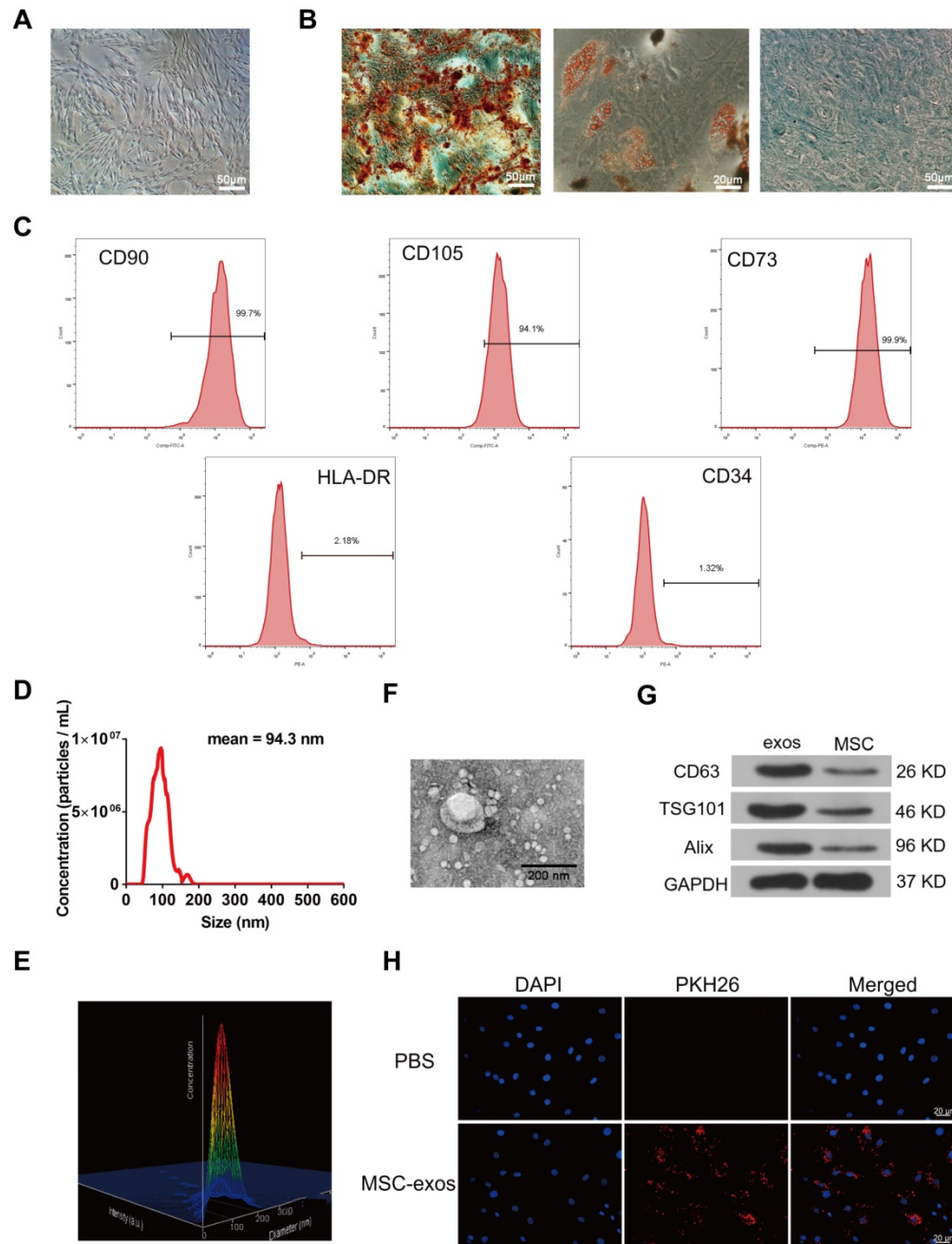


Figure 2. Identification of human bone marrow MSC and exosomes (MSC-exos). (A) Representative images of MSC spindle-like morphology and adherence to plastic (scale bar: 50 µm). (B) The ability of MSC to differentiate into the osteogenic, chondrogenic, and adipogenic lineages was confirmed by Alizarin Red staining (left panel, scale bar: 50 µm), Oil Red O staining (middle panel, scale bar: 20 µm) and Alcian blue staining (right panel, scale bar: 50 µm), respectively. (C) Cell surface markers (CD90, CD105, CD73, CD34 and HLA-DR) of MSC was detected by flow cytometric analysis. (D) Particle size distribution of MSC-exos was measured by nanoparticle trafficking analysis (NTA). (E) A three-dimensional plot according to the NTA results showed the stereo picture of MSC-exos size distribution. (F) Typical image of MSC-exos morphology was captured by transmission electron microscopy (TEM) (Scale bar: 200 nm). (G) Protein markers of MSC-exos were detected by western blot analysis in exosomes and MSC cells. (H) Representative images of NP cells incubated with PBS or PKH26-labelled MSC-exos for 12 h. The nuclei of NP cells were stained by DAPI (blue). Magnification: 400 ×, scale bar: 20 µm.

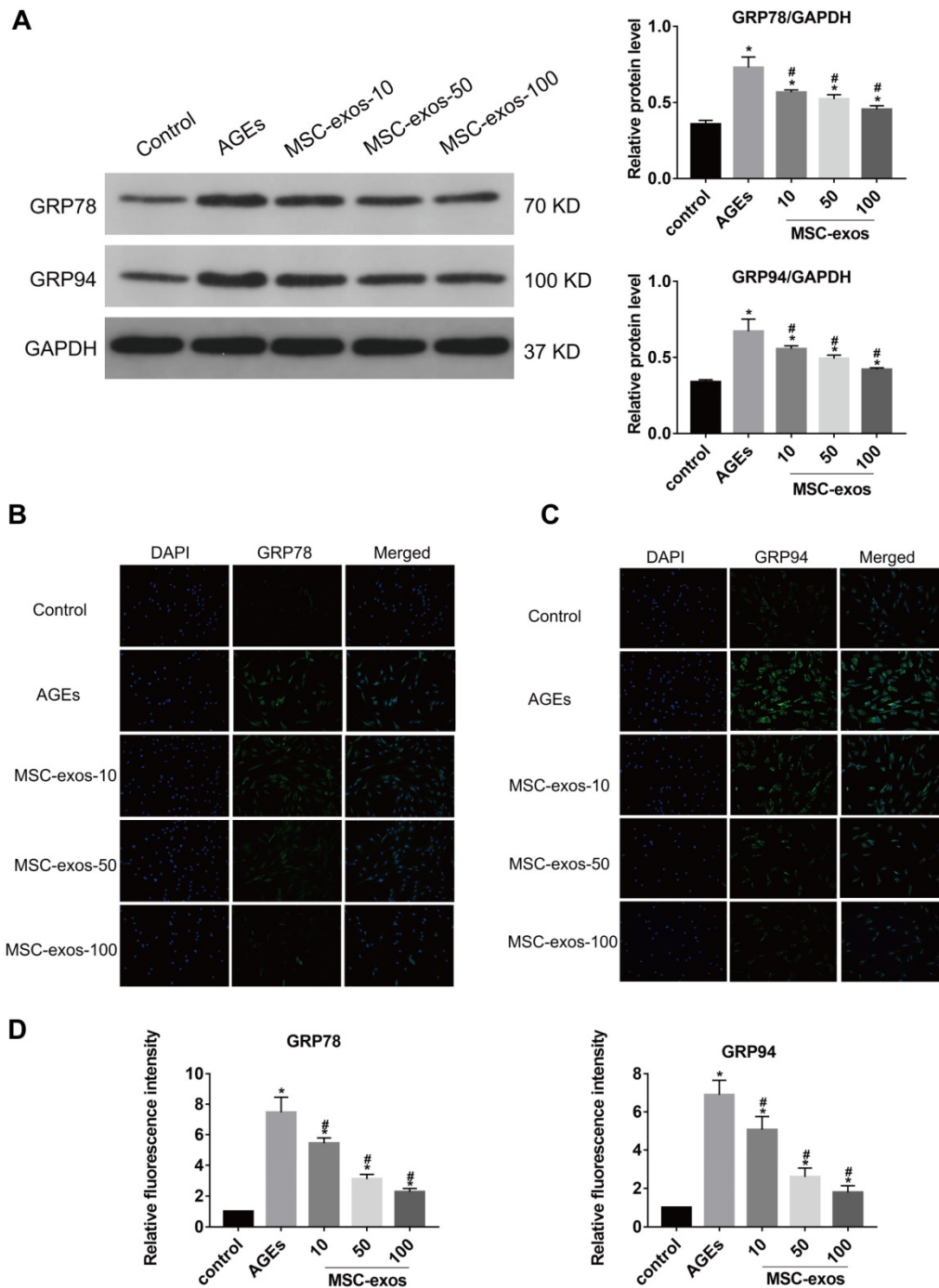


Figure 3. MSC-exos reduced the GRP78 and GRP94 expression under the AGEs stimulation. The human NP cells were treated with AGEs (200 µg/mL in 24 h except for in the control group. MSC-exos-10, 50, 100 indicates that 10, 50 or 100 µg/mL exosomes were used in the corresponding groups. (A) The protein levels of GRP78 and GRP94 were measured by western blot analysis and the relative quantitative data was calculated accordingly. GAPDH was used as an internal control. (B) Representative images of GRP78 expression treated with different concentrations of MSC-exos under the stimulation of AGEs. The nuclei of NP cells were stained by DAPI. Magnification: 200 ×. (C) Representative images of GRP94 expression in different groups. The nuclei of NP cells were stained by DAPI. Magnification: 200 ×. (D) Quantitative analysis of fluorescence intensity using Image-Pro Plus 6.0 for GRP78 and GRP94 according to the immunofluorescence analysis results. Data were presented as the mean ± SD. *P < 0.05 vs. control group, #P < 0.05 vs. AGEs group.

MSC-exos protected against AGEs-induced ER stress-induced apoptosis through AKT and ERK pathway in human NP cells

Numerous studies have confirmed that AKT and ERK pathways could be activated by the delivery of exosomes [36, 37]. To further investigate the

mechanism of MSC-exos in modulating ER stress, western blot analysis was carried out to measure the levels of AKT, p-AKT, ERK and p-ERK expression in human NP cells (Fig. 7A). The phosphorylated levels of AKT and ERK were both increased in the MSC-exos-treated group (100 µg/mL) compared with the AGEs group (Fig. 7B-C). The levels of CHOP

expression, caspase-3 and caspase-12 activation were also assessed by western blotting (Fig. 7D-G). Interestingly, the phosphorylation of both AKT and ERK was decreased under AGEs stimulation, and may be related to CHOP expression and caspase activation. MSC-exos treatment significantly activated the AKT and ERK signaling, which reduced CHOP expression and ultimately inhibited the cleavage of caspase-3 and caspase-12. However, the protective effects of MSC-exos were abrogated when the NP cells were treated with the AKT signaling inhibitor LY294002, or the ERK signaling inhibitor PD98059.

Immunofluorescence analysis also showed that the CHOP, caspase-3 and caspase-12-labeled cells decreased in the MSC-exos group, but increased significantly with LY294002 or PD98059 co-treatment (Fig. 7H). Moreover, the TUNEL staining results suggested that MSC-exos decreased the apoptotic rate, while blockade of AKT or ERK signaling inhibited the anti-apoptotic effects of MSC-exos *in vitro* (Fig. 7I-J). These results indicate that MSC-exos protect against ER stress-related apoptosis partly through the activation of AKT and ERK signaling in human NP cells.

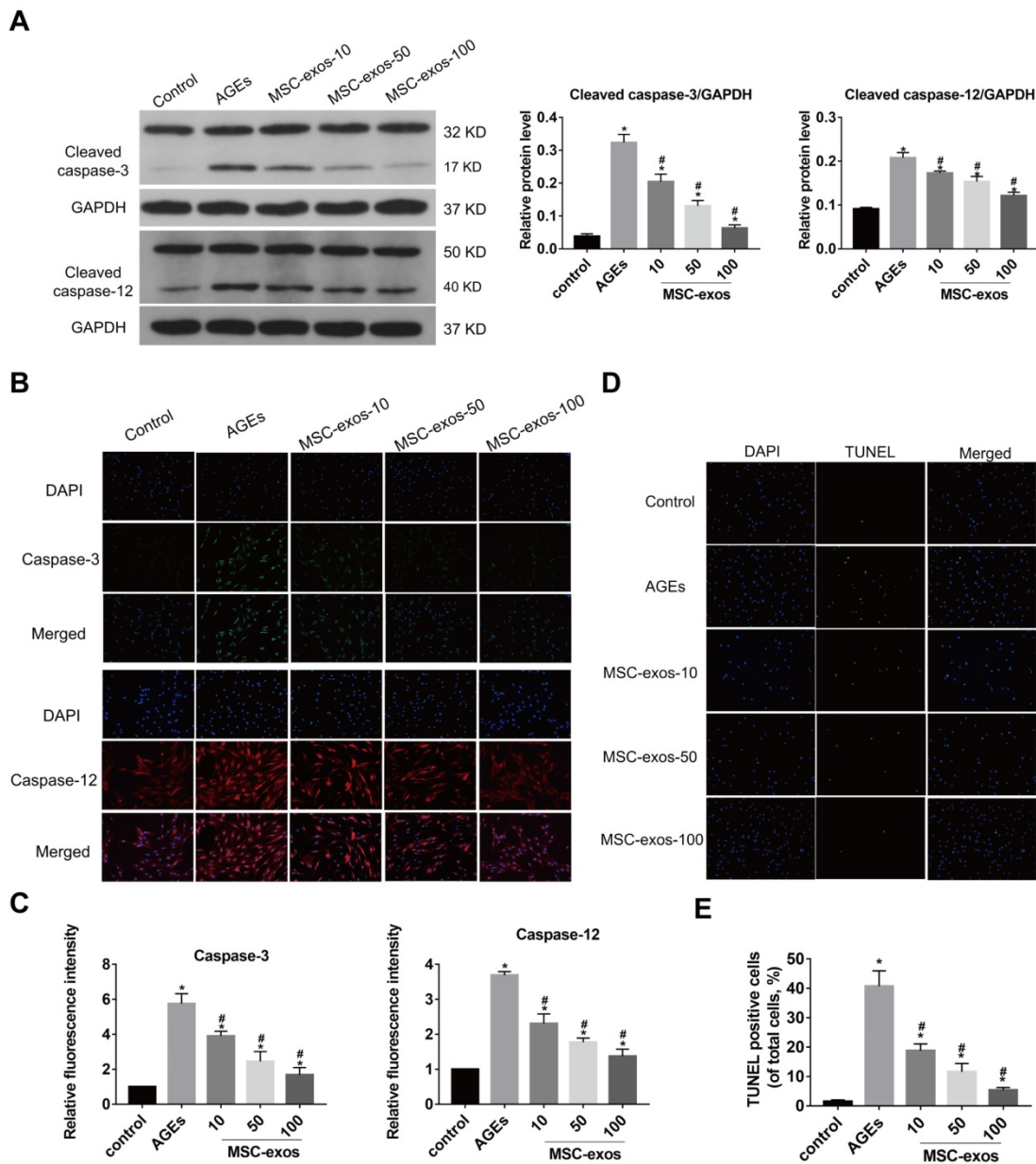


Figure 4. MSC-exos attenuated the activation of caspase-3 and caspase-12 under the AGEs stimulation in human NP cells. The human NP cells were treated with AGEs (200 µg/mL) in 24 h except for in the control group. MSC-exos-10, 50, 100 indicates that 10, 50 or 100 µg/mL exosomes were used in the corresponding groups. (A) Representative western blotting assay and quantitative analysis of cleaved caspase-3 and cleaved caspase-12 level. GAPDH was used as an internal control. (B) Representative images of caspase-3 and caspase-12 expression treated with different concentrations of MSC-exos under the stimulation of AGEs. The nuclei of NP cells were stained by DAPI. Magnification: 200 ×. (C) Quantitative analysis of fluorescence intensity for caspase-3 and caspase-12 according to the immunofluorescence analysis results. (D) Representative images of TUNEL analysis in different group. The nuclei of NP cells were stained by DAPI. Magnification: 200 ×. (E) Quantitation of the ratio of apoptotic cells in total cells was measured according to the TUNEL staining. Data were presented as the mean ± SD. *P < 0.05 vs. control group, #P < 0.05 vs. AGEs group.

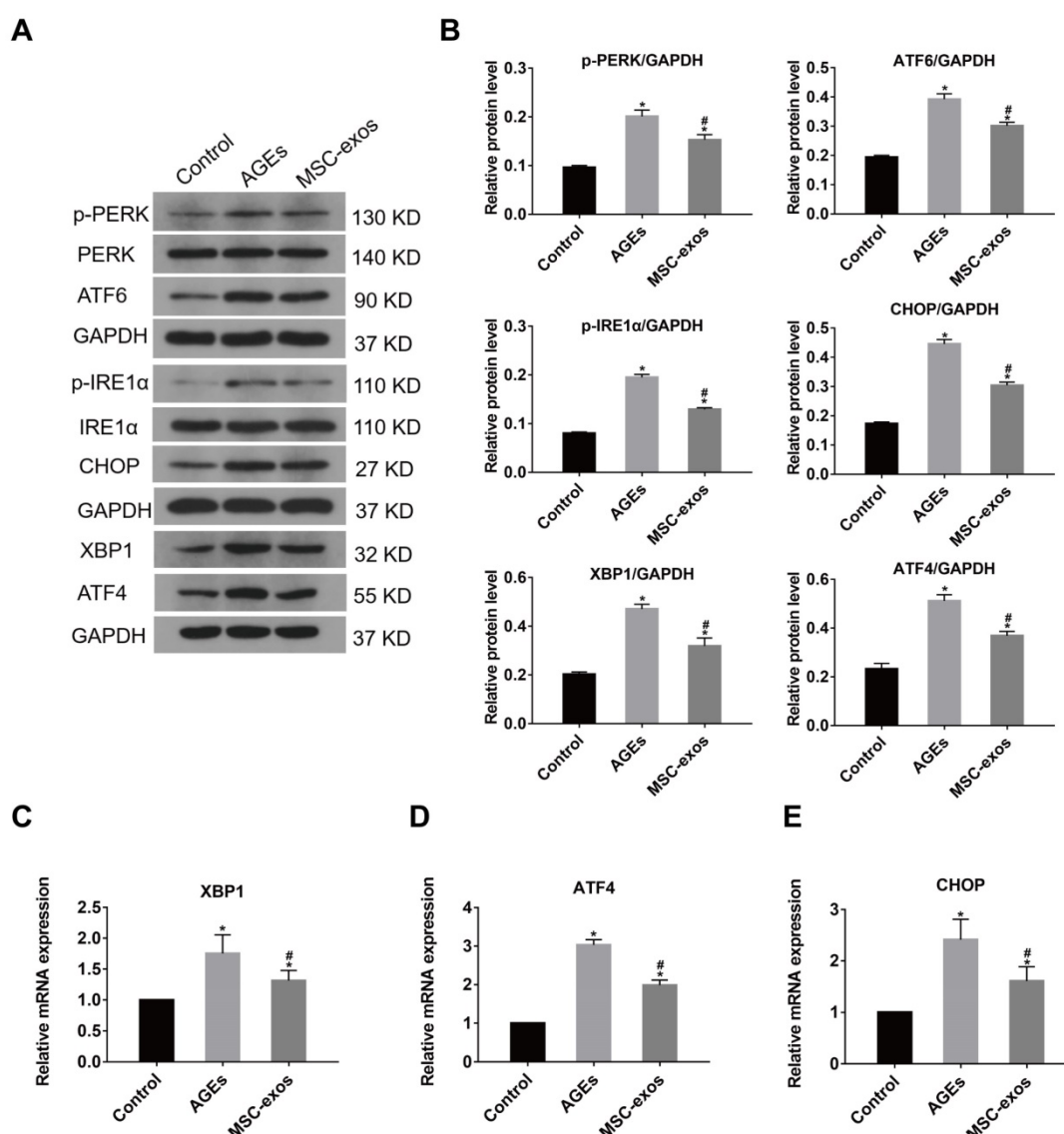


Figure 5. MSC-exos ameliorated the activation of UPR under the AGEs treatment. The MSC-exos group was cotreated with AGEs (200 µg/mL) and MSC-exos (100 µg/mL). (A) The protein expression levels of p-PERK, PERK, ATF6, p-IRE1α, IRE1α, XBP1, ATF4, and CHOP were measured by western blot analysis. GAPDH was used as an internal control. (B) Quantitative analysis of relative protein levels for p-PERK, ATF6, p-IRE1α, XBP1, ATF4, and CHOP. (C-E) The transcriptional levels of XBP1 (C), ATF4 (D) and CHOP (E) were analyzed by qRT-PCR. Data were presented as the mean ± SD. *P < 0.05 vs. control group, #P < 0.05 vs. AGEs group.

MSC-exos reduced ER stress-related cell apoptosis and ameliorated the intervertebral disc degeneration *in vivo*

To further investigate the therapeutic effects of MSC-exos on AGEs-induced IDD, an animal model of IDD was used in our experiment. Three independent discs of each rat were intradiscally injected with PBS, AGEs, or AGEs and MSC-exos, respectively. The degenerative grades of rat IVDs were assessed by MRI and X-ray examination at 0, 4 and 8 weeks after the intradiscal intervention (Fig. 8A-B). The percent disc height index (%DHI) was calculated according to the X-ray results (Fig. 8C). A low %DHI in AGEs-treated discs revealed degenerative changes indicating a collapsed or narrowing intervertebral space.

Meanwhile, the Pfirrmann score was based on MRI results, and was used to evaluate the degree of IDD, which was lower in the MSC-exos group compared with the AGEs group (Fig. 8D). Histological staining and immunohistochemical analysis for CHOP, GRP78 and caspase-3 also suggested that MSC-exos attenuated the AGEs-induced ER stress and cell apoptosis during IDD (Fig. 8E-F). Meanwhile, TUNEL staining revealed that the rate of TUNEL-positive cells was increased in the AGEs group and decreased significantly when discs were co-treated with AGEs and MSC-exos (Fig. 8G-H). Taken together, these results reveal that MSC-exos may inhibit the activation of AGEs-induced ER stress-related cell apoptosis and ameliorate IDD progression *in vivo*.

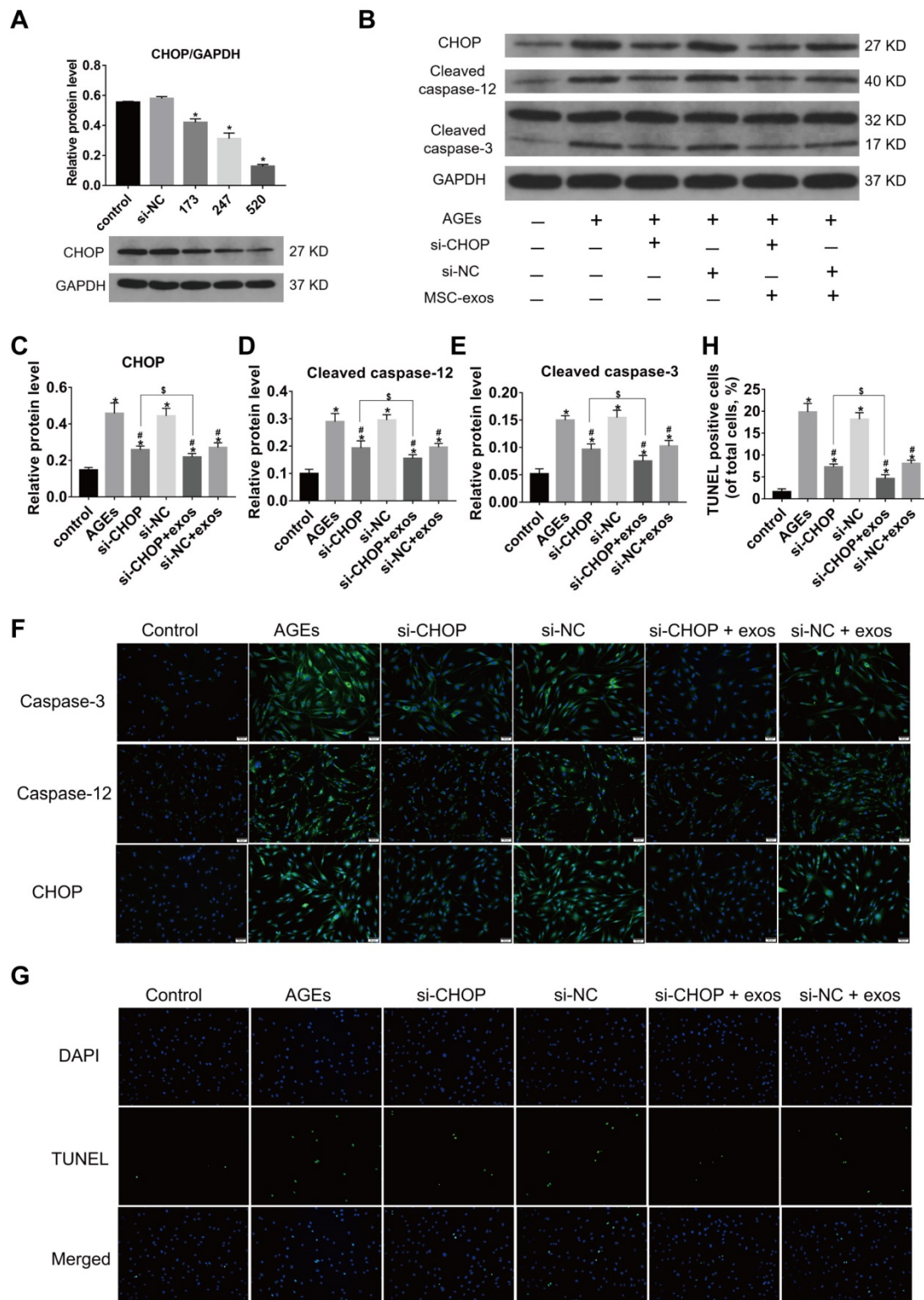


Figure 6. MSC-exos attenuated the AGEs-induced ER stress-induced apoptosis in human NP cells. The MSC-exos group was cotreated with AGEs (200 µg/mL) and MSC-exos (100 µg/mL). (A) Three fragments of si-CHOP (173, 247 and 520) were synthesized and the silencing efficiency was assessed by the western blotting analysis. Data were presented as the mean ± SD. *P < 0.05 vs. control group. (B-E) Western blot analysis and the quantitative statistical analysis showed the protein levels of CHOP (C), cleaved caspase-12 (D) and cleaved caspase-3 (E) expression. GAPDH was used as an internal control. Data were presented as the mean ± SD. *P < 0.05 vs. control group, #P < 0.05 vs. AGEs group, §P < 0.05. (F) Representative images of caspase-3, caspase-12 and CHOP protein expression were detected by immunofluorescence staining. Magnification: 200 ×. (G-H) Representative images of TUNEL staining (G) and the quantitative statistical analysis (H) showed the rate of TUNEL-positive cells in different groups. Magnification: 200 ×. Data were presented as the mean ± SD. *P < 0.05 vs. control group, #P < 0.05 vs. AGEs group, §P < 0.05.

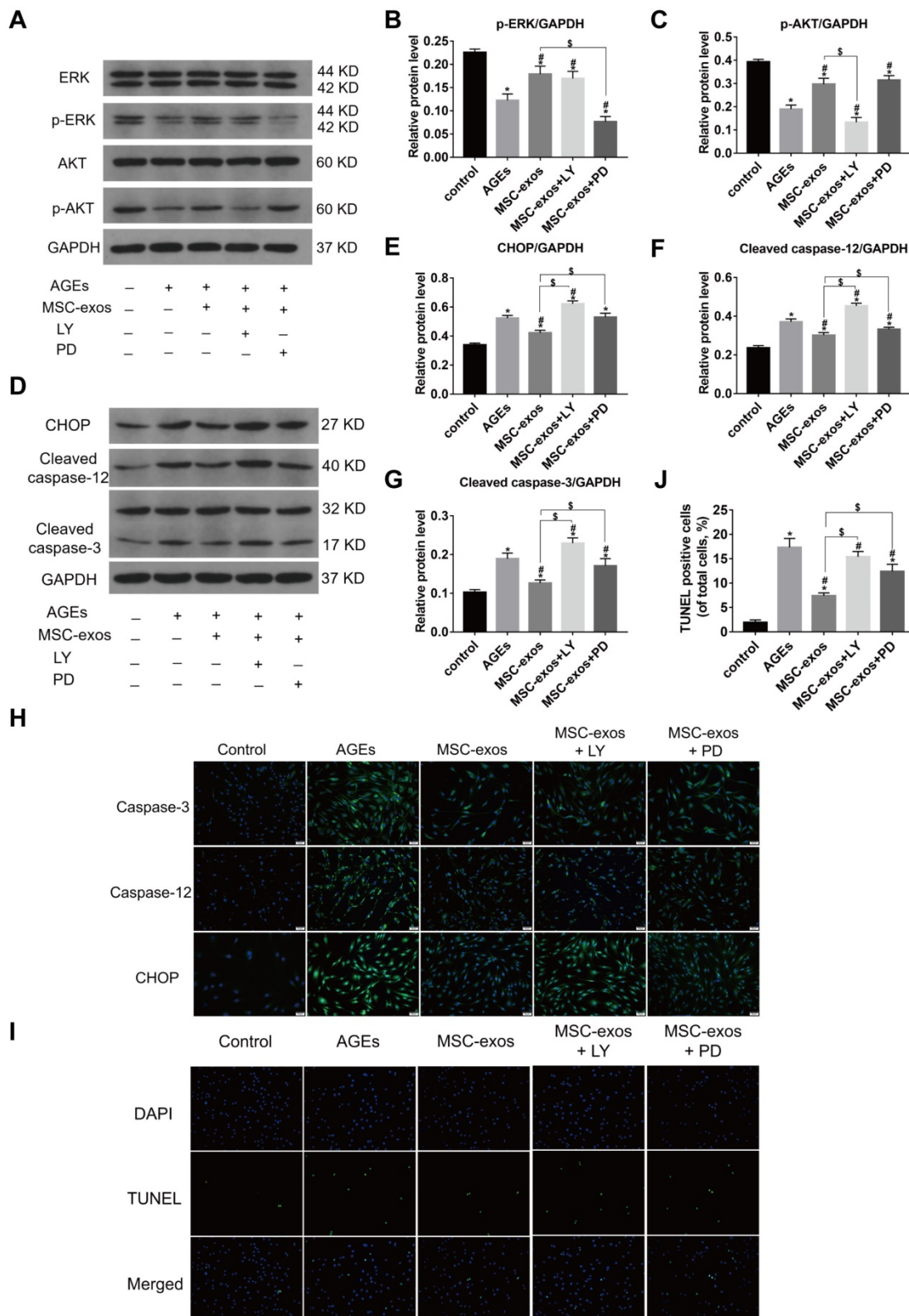


Figure 7. MSC-exos modulated the AGEs-induced ER stress through activating the AKT and ERK signaling in human NP cells. The MSC-exos group was cotreated with AGEs (200 µg/mL) and MSC-exos (100 µg/mL). (A) The protein levels of AKT, p-AKT, ERK and p-ERK were assessed by western blotting. LY294002 (LY) is a broad-spectrum inhibitor of PI3K/AKT. PD98059 (PD) could inhibit the phosphorylation of ERK 1/2 efficiently. (B-C) Western blot analysis and the quantitative statistical analysis showed the protein levels of p-AKT (B) and p-ERK (C). (D-G) The protein levels of CHOP (E), cleaved caspase-12 (F), cleaved-caspase-3 (G) were measured by western blotting and analyzed statistically. GAPDH was used as an internal control. Data were presented as the mean ± SD. *P < 0.05 vs. control group, #P < 0.05 vs. AGEs group, \$P < 0.05. (H) Representative images of caspase-3, caspase-12 and CHOP protein expression were assessed by immunofluorescence staining. Magnification: 200 ×. (I-J) Representative images of TUNEL staining (I) and the quantitative statistical analysis (J) showed the rate of TUNEL-positive cells in different groups. Magnification: 200 ×. Data were presented as the mean ± SD. *P < 0.05 vs. control group, #P < 0.05 vs. AGEs group, \$P < 0.05.

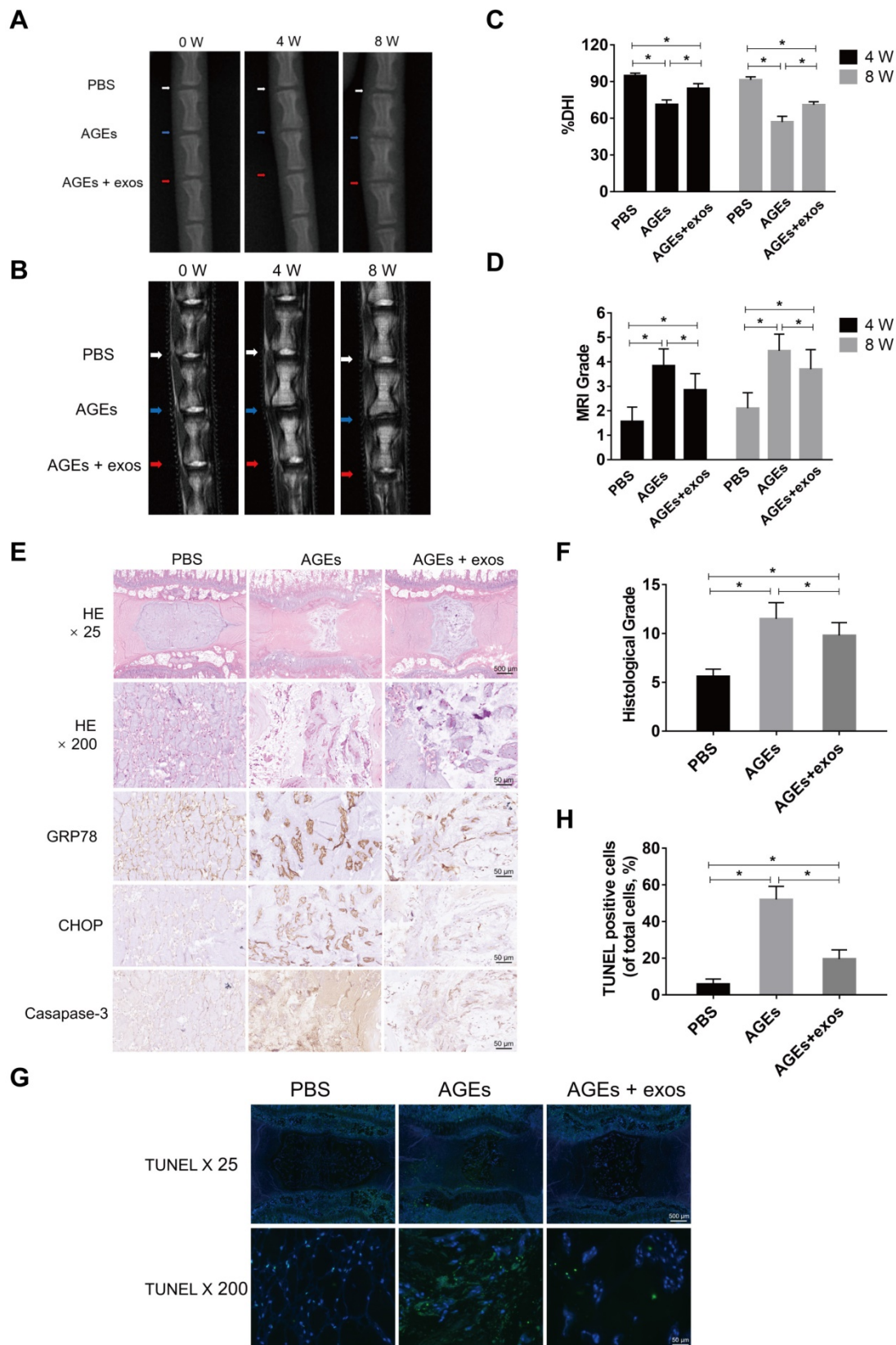


Figure 8. MSC-exos ameliorated the ER stress-related apoptosis and retarded the IDD progression in vivo. (A) X-ray of rat tail with three independent discs at 0, 4, 8 weeks. White, blue and red arrows mean discs with PBS, AGEs or AGEs and MSC-exos injection respectively. (B) T2-weighted MRI of rat tail at 0, 4, 8 weeks. White, blue and red arrows mean discs with PBS, AGEs or AGEs and MSC-exos injection respectively. (C-D) Changes in DHI (%DHI) (C) based on the X-ray and Pfirrmann MRI grades (D) based on the MRI results in each group (n = 20 for each group). Data were presented as the mean ± SD. *P < 0.05. (E) Representative HE staining and immunohistochemical staining of GRP78, CHOP and caspase-3 expression in each group. Magnification: 25 × (scar bar = 500 μm) and 200 × (scar bar = 50 μm). (F) Histological grades were assessed according to the HE staining (n = 20 for each group). Data were presented as the mean ± SD. *P < 0.05. (G-H) Representative TUNEL staining images (G) of rat discs and the statistical analysis (H) of TUNEL-positive cells in each group. Data were presented as the mean ± SD. *P < 0.05.

Discussion

Accumulating evidence has shown that MSC transplantation could ameliorate IDD progression through paracrine effects [21, 38]. Exosomes are a critical bioactive component of MSC secretion and may serve as an alternative to MSC-based therapy. In this study, we found that MSC-exos could protect NP cells against ER stress-induced apoptosis under the stimulation of AGEs in a dose-dependent manner. The anti-apoptotic effect of MSC-exos is partly mediated by the activation of AKT and ERK signaling through the inhibition of hyperactive ER stress and the UPR. Severe ER stress was induced by AGEs treatment and resulted in an accumulation of CHOP protein, which promoted the cleavage of caspase-12, caspase-3 in human NP cells. The supplementation with MSC-exos could attenuate the detrimental effects of AGEs in human NP cells. In addition, the *in vivo* study indicated that MSC-exos could ameliorate ER stress and play a protective role during IDD progression.

Both AGEs and ER stress play important roles in the pathogenesis of IDD. Higher level of AGEs was detected in the degenerated disc, especially in individuals with diabetes mellitus [15, 18]. AGEs accumulation was related to hyperactive inflammation, diminished glycosaminoglycan, and loss of water content in IVD tissues [7, 15, 16, 39]. Our previous study also showed that AGEs promoted human NP cell death and IDD progression through aggravating oxidative stress and mitochondrial dysfunction [18]. Moreover, AGEs accumulation was demonstrated to induce ER stress, leading to cell apoptosis mainly through the induction of a prolonged UPR [40]. Our results revealed that the levels of GRP78 and CHOP expression were increased in degenerative disc tissues, indicating an increasing ER stress level in parallel with the accumulation of AGEs during IDD progression. The *in vitro* study also found that GRP78 and GRP94 were both up-regulated significantly in AGEs-treated human NP cells compared with the normal control. Collectively, AGEs accumulation in the IVD promoted the progression of IDD partly through inducing a prolonged and severe ER stress. Studies in diabetic mice have revealed that AGEs accumulation is associated with degenerative changes in IVD, including hyperactive extracellular matrix catabolism, loss of disc height and diminished water content [39]. Inhibition of AGEs deposition and AGEs-related ER stress may provide a therapeutic target in IDD treatment.

The UPR, an evolutionarily conserved response induced by ER stress, could be activated to facilitate

cells to adapt to ER stress and survive in stressful conditions [41]. However, severe or prolonged ER stress promotes UPR hyperactivation to result in excessive cellular proteins degradation and the final demise of the cell [10]. The UPR is triggered to elicit downstream cascades, including ATF4 and XBP1, which contribute to the expression of CHOP protein [8, 12, 13, 42]. The accumulation of CHOP protein could induce the cleavage of caspase-12 and caspase-3, resulting in cell apoptosis [11, 43]. A previous study has indicated that CHOP deletion could ameliorate ER stress and abrogate the pro-apoptotic effects induced by the accumulation of AGEs in chondrocytes [44]. On the other hand, CHOP overexpression was found to promote the activation of caspase-3 and cause an increased apoptotic rate [45]. Our discoveries revealed that knockdown of CHOP by si-RNA in human NP cells attenuated the activation of caspase-12 and caspase-3, and alleviated the ER stress-induced apoptosis.

MSC transplantation has been proposed as an ideal approach for IVD regeneration because MSCs could protect against resident IVD cell death through the paracrine effects [46]. MSC-exos, as a component of MSC paracrine, could serve as an alternative to stem cell-based therapy [47]. Moreover, exosomes-based therapy could be applied between different individuals, even across species [48, 49]. MSC-exos have been applied in immunomodulation, wound healing, mediating inflammation and cell apoptosis regulation [36, 37, 50, 51]. In our study, accumulation of AGEs was found to promote CHOP expression and impaired NP cells. Treatment with MSC-exos ameliorated the UPR hyperactivation and decreased CHOP expression, which protected NP cells against excessive apoptosis ultimately. When cells were treated with an AKT antagonist or ERK antagonist, the anti-apoptotic effects of MSC-exos were significantly abrogated. These results indicate that MSC-exos could decrease the level of CHOP expression and reduce caspase activation in a severe ER stress condition.

To date, exosomes are known as a conveyor to deliver cargoes from the parental cells to the recipient cells. The therapeutic mechanisms of MSC-exos could be explained by transmission of bioactive factors from MSCs to target cells through a stable bilayer membrane structure. Accumulating evidence has revealed that exosomal proteins or RNAs play a significant role in altering the cellular activities and functions of recipient cells [24, 25]. A recent study showed that exosomes from blood plasma could activate the AKT and ERK pathways to regulate angiogenesis and promote the expression of anti-apoptotic proteins [37]. Exosomal proteins, such

as CD73, were found to mediate the activation of AKT and ERK signaling [52]. AKT and ERK signaling are involved in cell proliferation and migration, and play a great role in the regulation of protein synthesis, cell apoptosis, and metabolism [52-54]. Impairing the AKT and ERK pathways was found to aggravate ER stress-related apoptosis and mitochondrial dysfunction [35]. Treatment with AGEs induced CHOP expression and promoted the dephosphorylation of AKT and ERK according to our results. Moreover, administration of MSC-exos restored the impaired AKT and ERK signaling, resulting in a decreased apoptotic rate in human NP cells. However, the protective effects of MSC-exos were removed when cells were cotreated with the PI3K/AKT inhibitor LY294002, or the ERK inhibitor PD98059. CHOP and cleaved-caspase-3 expression were both increased when AKT or ERK signaling was blocked. Consequently, it is reasonable to suggest that MSC-exos ameliorated ER stress-induced apoptosis partly through the activation of the AKT and ERK signaling pathways.

We further investigated the role of MSC-exos in a rat tail model of IDD. Our previous study verified that disc injection of AGEs will trigger and accelerate IDD progression [18]. A suitable needle diameter and small injection volume will minimize the influence of the injection itself on IDD. In our study, we used a 33-gauge needle for the delivery of MSC-exos, with a volume of 2 μ L, in order to not accelerate the IDD process [31, 32]. In line with the results of our *in vitro* studies, the *in vivo* study also showed that MSC-exos were effective in ameliorating ER stress-related apoptosis in NP cells. Consistent with the profile of AGEs level, the expression of GRP78 and CHOP was increased in degenerative IVD tissues which indicated a prolonged ER stress condition during IDD progression. Treatment with MSC-exos decreased the expression of CHOP and GRP78, and ameliorated the IDD progression to some degree, according to histological assessment. Collectively, MSC-exos protected against NP cells apoptosis induced by AGEs and showed promise in retarding IDD progression.

Exosomes derived from MSC have been testified the therapeutic potential in IVD regeneration. A recent study showed that MSC-exos could promote NP cell proliferation and enhance extracellular matrix production *in vitro* [23]. In addition, Cheng et al. found that MSC-exos inhibited NP cell apoptosis through the transfer of exosomal microRNA targeting on activating PI3K/AKT pathway [22]. In our study, we investigated the role of MSC-exos in ameliorating ER stress-induced apoptosis in human NP cells. Consistent with previous studies, we verified the therapeutic effects of MSC-exos on the IDD process.

However, there are still some limitations with our study. Although our study found that the MSC-exos intervention attenuated ER stress-related apoptosis in NP cells through AKT and ERK signaling, further investigation is required to fully reveal the underlying mechanisms in MSC-exos modulation of ER stress. In addition, though the rat model used in our study could simulate the pathological development of IDD to some degree, the IVDs of rodents are different from mammals in both functional and biomechanical traits. Studies using IDD models involved in pigs, monkeys or goats are required in the further research.

In summary, we demonstrated that the levels of ER stress markers and cell apoptosis are increased during IDD. MSC-exos could ameliorate ER stress-induced NP cells apoptosis under the AGEs stimulation *in vitro*. In addition, the transfer of MSC-exos into the disc could attenuate ER stress-related apoptosis during IDD and may reverse IDD progression *in vivo*. These findings offer new therapeutic opportunities for extracellular vesicles or exosomes in the treatment of IVD degeneration.

Abbreviations

IDD, intervertebral disc degeneration; IVD, intervertebral disc; NP, nucleus pulposus; AF, annulus fibrosus; ECM, extracellular matrix; AGEs, advanced glycation end products; ER, endoplasmic reticulum; UPR, unfolded protein response; CHOP, C/EBP homologous protein; MSC, mesenchymal stem cells; MSC-exos, exosomes derived from MSC; AKT, serine-threonine protein kinase; ERK, extracellular signal-regulated kinase; GRP78, binding immunoglobulin protein; GRP94, heat shock protein 90kDa beta member 1; CD73, cluster of differentiation 73; CD90, cluster of differentiation 90; CD105, cluster of differentiation 105; CD34, cluster of differentiation 34; HLA-DR, human leukocyte antigen-DR isotype; CD63, cluster of differentiation 63; TSG101, tumor susceptibility gene 101; Alix, programmed cell death 6-interacting protein; PERK, protein kinase-like endoplasmic reticulum kinase; IRE1 α , inositol-requiring protein 1 α ; ATF6, activating transcription factor 6; ATF4, activating transcription factor 4; XBP1, X-box binding protein 1.

Acknowledgements

This study was supported by the National Key Research and Development Program of China (2018YFB1105700), the National Natural Science Foundation of China (U1603121, 81772401) and Natural Science Foundation of Hubei Province (WJ2017Z016).

Competing Interests

The authors have declared that no competing interest exists.

References

- Priyadarshani P, Li Y, Yao L. Advances in biological therapy for nucleus pulposus regeneration. *Osteoarthritis Cartilage*. 2016; 24: 206-12.
- Verfaillie T, Garg AD, Agostinis P. Targeting ER stress induced apoptosis and inflammation in cancer. *Cancer Lett*. 2013; 332: 249-64.
- Vergroesen PP, Kingma I, Emanuel KS, Hoogendoorn RJ, Welting TJ, van Royen BJ, et al. Mechanics and biology in intervertebral disc degeneration: a vicious circle. *Osteoarthritis Cartilage*. 2015; 23: 1057-70.
- Chan CM, Huang DY, Huang YP, Hsu SH, Kang LY, Shen CM, et al. Methylglyoxal induces cell death through endoplasmic reticulum stress-associated ROS production and mitochondrial dysfunction. *J Cell Mol Med*. 2016; 20: 1749-60.
- Nowotny K, Castro JP, Hugo M, Braune S, Weber D, Pignitter M, et al. Oxidants produced by methylglyoxal-modified collagen trigger ER stress and apoptosis in skin fibroblasts. *Free Radic Biol Med*. 2018; 120: 102-13.
- Chiang CK, Wang CC, Lu TF, Huang KH, Sheu ML, Liu SH, et al. Involvement of Endoplasmic Reticulum Stress, Autophagy, and Apoptosis in Advanced Glycation End Products-Induced Glomerular Mesangial Cell Injury. *Sci Rep*. 2016; 6: 34167.
- Song Y, Wang Y, Zhang Y, Geng W, Liu W, Gao Y, et al. Advanced glycation end products regulate anabolic and catabolic activities via NLRP3-inflammasome activation in human nucleus pulposus cells. *J Cell Mol Med*. 2017; 21: 1373-87.
- Guo R, Liu W, Liu B, Zhang B, Li W, Xu Y. SIRT1 suppresses cardiomyocyte apoptosis in diabetic cardiomyopathy: An insight into endoplasmic reticulum stress response mechanism. *Int J Cardiol*. 2015; 191: 36-45.
- Liu J, Huang K, Cai GY, Chen XM, Yang JR, Lin LR, et al. Receptor for advanced glycation end-products promotes premature senescence of proximal tubular epithelial cells via activation of endoplasmic reticulum stress-dependent p21 signaling. *Cell Signal*. 2014; 26: 110-21.
- Kim I, Xu W, Reed JC. Cell death and endoplasmic reticulum stress: disease relevance and therapeutic opportunities. *Nat Rev Drug Discov*. 2008; 7: 1013-30.
- Hirsch I, Weiwad M, Prell E, Ferrari DM. ERp29 deficiency affects sensitivity to apoptosis via impairment of the ATF6-CHOP pathway of stress response. *Apoptosis*. 2014; 19: 801-15.
- Senkal CE, Ponnusamy S, Bielawski J, Hannun YA, Ogretmen B. Antiapoptotic roles of ceramide-synthase-6-generated C16-ceramide via selective regulation of the ATF6/CHOP arm of ER-stress-response pathways. *FASEB J*. 2010; 24: 296-308.
- Xu Z, Bu Y, Chitnis N, Koumenis C, Fuchs SY, Diehl JA. miR-216b regulation of c-Jun mediates GADD153/CHOP-dependent apoptosis. *Nat Commun*. 2016; 7: 11422.
- Zhang YH, Zhao CQ, Jiang LS, Dai LY. Lentiviral shRNA silencing of CHOP inhibits apoptosis induced by cyclic stretch in rat annular cells and attenuates disc degeneration in the rats. *Apoptosis*. 2011; 16: 594-605.
- Fields AJ, Berg-Johansen B, Metz LN, Miller S, La B, Liebenberg EC, et al. Alterations in intervertebral disc composition, matrix homeostasis and biomechanical behavior in the UCD-T2DM rat model of type 2 diabetes. *J Orthop Res*. 2015; 33: 738-46.
- Jazini E, Sharan AD, Morse LJ, Dyke JP, Aronowitz EB, Chen LK, et al. Alterations in T2 relaxation magnetic resonance imaging of the ovine intervertebral disc due to nonenzymatic glycation. *Spine*. 2012; 37: E209-15.
- Yoshida T, Park JS, Yokosuka K, Jimbo K, Yamada K, Sato K, et al. Up-regulation in receptor for advanced glycation end-products in inflammatory circumstances in bovine coccygeal intervertebral disc specimens in vitro. *Spine*. 2009; 34: 1544-8.
- Song Y, Li S, Geng W, Luo R, Liu W, Tu J, et al. Sirtuin 3-dependent mitochondrial redox homeostasis protects against AGEs-induced intervertebral disc degeneration. *Redox Biol*. 2018; 19: 339-53.
- Chen S, Zhao L, Deng X, Shi D, Wu F, Liang H, et al. Mesenchymal Stem Cells Protect Nucleus Pulposus Cells from Compression-Induced Apoptosis by Inhibiting the Mitochondrial Pathway. *Stem Cells Int*. 2017; 2017: 9843120.
- Henry N, Clouet J, Le Bideau J, Le Visage C, Guicheux J. Innovative strategies for intervertebral disc regenerative medicine: From cell therapies to multiscale delivery systems. *Biotechnol Adv*. 2018; 36: 281-94.
- Yang F, Leung VY, Luk KD, Chan D, Cheung KM. Mesenchymal stem cells arrest intervertebral disc degeneration through chondrocytic differentiation and stimulation of endogenous cells. *Mol Ther*. 2009; 17: 1959-66.
- Cheng X, Zhang G, Zhang L, Hu Y, Zhang K, Sun X, et al. Mesenchymal stem cells deliver exogenous miR-21 via exosomes to inhibit nucleus pulposus cell apoptosis and reduce intervertebral disc degeneration. *J Cell Mol Med*. 2018; 22: 261-76.
- Lu K, Li HY, Yang K, Wu JL, Cai XW, Zhou Y, et al. Exosomes as potential alternatives to stem cell therapy for intervertebral disc degeneration: in-vitro study on exosomes in interaction of nucleus pulposus cells and bone marrow mesenchymal stem cells. *Stem cell research & therapy*. 2017; 8: 108.
- Rani S, Ryan AE, Griffin MD, Ritter T. Mesenchymal Stem Cell-derived Extracellular Vesicles: Toward Cell-free Therapeutic Applications. *Mol Ther*. 2015; 23: 812-23.
- Lai RC, Yeo RW, Lim SK. Mesenchymal stem cell exosomes. *Semin Cell Dev Biol*. 2015; 40: 82-8.
- Willms E, Cabanas C, Mager I, Wood MJA, Vader P. Extracellular Vesicle Heterogeneity: Subpopulations, Isolation Techniques, and Diverse Functions in Cancer Progression. *Front Immunol*. 2018; 9: 738.
- Phinney DG, Pittenger MF. Concise Review: MSC-Derived Exosomes for Cell-Free Therapy. *Stem Cells*. 2017; 35: 851-8.
- Chang YH, Wu KC, Harn HJ, Lin SZ, Ding DC. Exosomes and Stem Cells in Degenerative Disease Diagnosis and Therapy. *Cell Transplant*. 2018; 27: 349-63.
- Barile L, Vassalli G. Exosomes: Therapy delivery tools and biomarkers of diseases. *Pharmacol Ther*. 2017; 174: 63-78.
- Wu X, Song Y, Liu W, Wang K, Gao Y, Li S, et al. IAPP modulates cellular autophagy, apoptosis, and extracellular matrix metabolism in human intervertebral disc cells. *Cell Death Discov*. 2017; 3: 16107.
- Elliott DM, Yerramalli CS, Beckstein JC, Boxberger JJ, Johannessen W, Vresilovic EJ. The effect of relative needle diameter in puncture and sham injection animal models of degeneration. *Spine*. 2008; 33: 588-96.
- Mao HJ, Chen QX, Han B, Li FC, Feng J, Shi ZL, et al. The effect of injection volume on disc degeneration in a rat tail model. *Spine*. 2011; 36: E1062-9.
- Han B, Zhu K, Li FC, Xiao YX, Feng J, Shi ZL, et al. A simple disc degeneration model induced by percutaneous needle puncture in the rat tail. *Spine*. 2008; 33: 1925-34.
- Fujii T, Fujita N, Suzuki S, Tsuji T, Takaki T, Umezawa K, et al. The unfolded protein response mediated by PERK is casually related to the pathogenesis of intervertebral disc degeneration. *J Orthop Res*. 2018; 36: 1334-45.
- Xu D, Jin H, Wen J, Chen J, Chen D, Cai N, et al. Hydrogen sulfide protects against endoplasmic reticulum stress and mitochondrial injury in nucleus pulposus cells and ameliorates intervertebral disc degeneration. *Pharmacol Res*. 2017; 117: 357-69.
- Guo SC, Tao SC, Yin WJ, Qi X, Yuan T, Zhang CQ. Exosomes derived from platelet-rich plasma promote the re-epithelization of chronic cutaneous wounds via activation of YAP in a diabetic rat model. *Theranostics*. 2017; 7: 81-96.
- Tao SC, Yuan T, Rui BY, Zhu ZZ, Guo SC, Zhang CQ. Exosomes derived from human platelet-rich plasma prevent apoptosis induced by glucocorticoid-associated endoplasmic reticulum stress in rat osteonecrosis of the femoral head via the Akt/Bad/Bcl-2 signal pathway. *Theranostics*. 2017; 7: 733-50.
- Leung VY, Aladin DM, Lv F, Tam V, Sun Y, Lau RY, et al. Mesenchymal stem cells reduce intervertebral disc fibrosis and facilitate repair. *Stem Cells*. 2014; 32: 2164-77.
- Illien-Junger S, Grosjean F, Laudier DM, Vlassara H, Striker GE, Iatridis JC. Combined anti-inflammatory and anti-AGE drug treatments have a protective effect on intervertebral discs in mice with diabetes. *PLoS One*. 2013; 8: e64302.
- Adamopoulos C, Mihailidou C, Grivaki C, Papavassiliou KA, Kiaris H, Piperi C, et al. Systemic effects of AGEs in ER stress induction in vivo. *Glycoconj J*. 2016; 33: 537-44.
- Hetz C. The unfolded protein response: controlling cell fate decisions under ER stress and beyond. *Nature Reviews Molecular Cell Biology*. 2012; 13: 89-102.
- Szegezdi E, Logue SE, Gorman AM, Samali A. Mediators of endoplasmic reticulum stress-induced apoptosis. *EMBO Rep*. 2006; 7: 880-5.
- Go BS, Kim J, Yang JH, Choe ES. Psychostimulant-Induced Endoplasmic Reticulum Stress and Neurodegeneration. *Molecular neurobiology*. 2017; 54: 4041-8.
- Yamabe S, Hirose J, Uehara Y, Okada T, Okamoto N, Oka K, et al. Intracellular accumulation of advanced glycation end products induces apoptosis via endoplasmic reticulum stress in chondrocytes. *FEBS J*. 2013; 280: 1617-29.
- Ding X, Ma M, Teng J, Shao F, Wu E, Wang X. Numb Protects Human Renal Tubular Epithelial Cells From Bovine Serum Albumin-Induced Apoptosis Through Antagonizing CHOP/PERK Pathway. *J Cell Biochem*. 2016; 117: 163-71.
- Richardson SM, Kalamegam G, Pushparaj PN, Matta C, Memic A, Khademhosseini A, et al. Mesenchymal stem cells in regenerative medicine: Focus on articular cartilage and intervertebral disc regeneration. *Methods (San Diego, Calif)*. 2016; 99: 69-80.
- Meldolesi J. Exosomes and Ectosomes in Intercellular Communication. *Curr Biol*. 2018; 28: R435-R44.
- Monsel A, Zhu YG, Gennai S, Hao Q, Hu S, Rouby JJ, et al. Therapeutic Effects of Human Mesenchymal Stem Cell-derived Microvesicles in Severe Pneumonia in Mice. *American journal of respiratory and critical care medicine*. 2015; 192: 324-36.
- Toh WS, Lai RC, Hui JHP, Lim SK. MSC exosome as a cell-free MSC therapy for cartilage regeneration: Implications for osteoarthritis treatment. *Semin Cell Dev Biol*. 2017; 67: 56-64.
- Cosenza S, Toupet K, Maumus M, Luz-Crawford P, Blanc-Brude O, Jorgensen C, et al. Mesenchymal stem cells-derived exosomes are more immunosuppressive than microparticles in inflammatory arthritis. *Theranostics*. 2018; 8: 1399-410.

51. Zhang B, Wang M, Gong A, Zhang X, Wu X, Zhu Y, et al. HucMSC-Exosome Mediated-Wnt4 Signaling Is Required for Cutaneous Wound Healing. *Stem Cells*. 2015; 33: 2158-68.
52. Zhang S, Chuah SJ, Lai RC, Hui JHP, Lim SK, Toh WS. MSC exosomes mediate cartilage repair by enhancing proliferation, attenuating apoptosis and modulating immune reactivity. *Biomaterials*. 2018; 156: 16-27.
53. Zhu J, Yao J, Huang R, Wang Y, Jia M, Huang Y. Ghrelin promotes human non-small cell lung cancer A549 cell proliferation through PI3K/Akt/mTOR/P70S6K and ERK signaling pathways. *Biochemical and biophysical research communications*. 2018; 498: 616-20.
54. Xiao M, Tang Y, Chen WW, Wang YL, Yang L, Li X, et al. Tubb3 regulation by the Erk and Akt signaling pathways: a mechanism involved in the effect of arginine ADP-ribosyltransferase 1 (Art1) on apoptosis of colon carcinoma CT26 cells. *Tumour biology : the journal of the International Society for Oncodevelopmental Biology and Medicine*. 2016; 37: 2353-63.